Published by IOP Publishing for Sissa Medialab

Received: *January 23, 2022*
Revised: *June 21, 2022*
Accepted: *August 9, 2022*
Published: *September 6, 2022*

Comparative assessment of passive scattering and active scanning proton therapy techniques using Monte Carlo simulations

A. Asadi,[a] S.A. Hosseini,[a,*] A. Akhavanallaf,[b] N. Vosoughi[a] and H. Zaidi[b,c,d,e]

[a] *Department of Energy Engineering, Sharif University of Technology, Tehran, Iran*
[b] *Division of Nuclear Medicine and Molecular Imaging, Geneva University Hospital, CH-1211 Geneva 4, Switzerland*
[c] *Geneva University Neurocenter, Geneva University, CH-1205 Geneva, Switzerland*
[d] *Department of Nuclear Medicine and Molecular Imaging, University of Groningen, University Medical Center Groningen, 9700 RB Groningen, Netherlands*
[e] *Department of Nuclear Medicine, University of Southern Denmark, DK-500, Odense, Denmark*

E-mail: sahosseini@sharif.edu

Abstract: **Background:** in this study, two proton beam delivery designs, i.e. passive scattering proton therapy (PSPT) and pencil beam scanning (PBS), were quantitatively compared in terms of dosimetric indices. The GATE Monte Carlo (MC) particle transport code was used to simulate the proton beam system; and the developed simulation engines were benchmarked with respect to the experimental measurements.

Method: a water phantom was used to simulate system energy parameters using a set of depth-dose data in the energy range of 120–235 MeV. To compare the performance of PSPT against PBS, multiple dosimetric parameters including Bragg peak width (BP_{W50}), peak position, range, peak-to-entrance dose ratio, $penumbra_{(90-10)\%}$, $penumbra_{(80-20)\%}$, $M_{95\%}$ and dose volume histogram have been analyzed under the same conditions. Furthermore, the clinical test cases introduced by AAPM TG-119 were simulated in both beam delivery modes to compare the relevant clinical values obtained from Dose Volume Histogram (DVH) analysis.

Results: the parametric comparison in the water phantom between the two techniques revealed that the value of peak-to-entrance dose ratio in PSPT is considerably higher than that from PBS by a factor of 8%. In addition, the BP_{W50}, $penumbra_{(90-10)\%}$, $penumbra_{(80-20)\%}$, and $M_{95\%}$ in PSPT

*Corresponding author.

https://doi.org/10.1088/1748-0221/17/09/P09008

was increased by a factor of 7, 51, 37, and 2.7%, respectively compared to the corresponding value obtained from PBS model. TG-119 phantom simulations showed that the difference of PTV mean dose between PBS and PSPT techniques are up to 1.8% while the difference of max dose to organ at risks (OARs) exceeds 50%.

Conclusion: the results of this simulation show that although the passive scattering design method has a slightly higher ability to adjust the dose in target volume, but the active scanning proton therapy systems was superior in dose painting, and lower out-of-field dose compared to passive scattering design.

KEYWORDS: Instrumentation for particle-beam therapy; Beam-line instrumentation (beam position and profile monitors, beam-intensity monitors, bunch length monitors); Instrumentation for heavy-ion accelerators; Targets (spallation source targets, radioisotope production, neutrino and muon sources)

ARXIV EPRINT: 2107.12185

2022 JINST 17 P09008

Contents

2022 JINST 17 P09008

1 Introduction

Proton therapy (PT) due to their excellent dose distribution can significantly reduce the absorbed dose by the patient's body relative to the photon beams [1]. PT was first initiated in 1954 and is currently going as part of modern radiation therapy technologies in many developed countries [2]. In PT, there are two main techniques of irradiation, namely active scanning or Pencil Beam Scanning (PBS) and Passive Scattering Proton Therapy (PSPT). Passive scattering facilities are composed of specific mechanical devices in the particle trajectory to shape the beam to the tumor volume using particle-matter interactions. The scattering interaction spread the originally Gaussian-distributed beam to shape a wide homogeneous beam to the tumor using patient-specific collimators. A rotating wheel of varying thickness, called range modulator, is used to generate a uniform Spread-Out Bragg Peak (SOBP). Lastly, proton beam travel through a longitudinal compensator, a specific scatterer device, specifically drilled for each field and each patient, to achieve the last conformal shaping of the beam just before the skin of the patient. Nowadays, proton beam delivery is switching from the use of passively scattered mode to pencil beam scanning owing to the feasibility of more conformal dose to tumors and higher dose rate in PBS compared to PSPT [3]. In addition, pencil beam technique can reduce the need for specific mechanical hardware required in PSPT. Another advantage of the active scanning technique is related to the lower level of secondary particles, mostly neutrons that are generated from the interaction of primary protons with multiple scattering components. In PBS, multiple magnets in x and y directions, based on the charge of particles, are used to drift the beam and scanning the target volume spot by spot with a 3D narrow pencil beam [4, 5]. There are some studies in biological dose comparison between active and passive scanning proton therapy techniques in the cellular level [3, 6, 7]. Gridley et al. [7] compared cell response to active scanning and

passive beam delivery techniques. They reported lower dose values at the entrance region, a sharper fall-off and a higher dose rate for active scanning mode. While they did not find any considerable difference in relative biological effectiveness (RBE) between two methods. Michaelidesova et al. [3] reported that between two techniques, there is neither considerable beam quality difference from MC simulation, nor statistically significant difference in biological endpoints. Nomura et al. [6] reported a higher Linear Energy Transfer (LET) at distal region in active scanning mode compared to passive scattering method. To the best of our knowledge, the current study is the first report that systematically compares physical doses between two modes of proton therapy. In this work, multiple dosimetric criteria such as BP_{W50}, peak position, range, peak-to-entrance dose ratio, $M_{95\%}$ (the distance between two points in the proximal and distal regions over which the dose falls to 95% of the average dose), penumbras, and etc. have been analyzed. Furthermore, clinically relevant dose parameters have been compared through TG-119 clinical test cases.

2 Material and method

2.1 Beam Modeling

In this work, two main proton therapy techniques, i.e. PBS and PSPT, have been simulated using GATE v8.2 MC code alongside with GEANT4 10.5 p01 [8–11]. Shanghai Advanced Proton Therapy (SAPT) facility, a synchrotron-based active scanning proton therapy system, was simulated. Fig 1. Depicts the geometrical characteristics of SIEMENS IONTRIS system at SAPT. In this system proton beams are extracted from synchrotron and drifted to the nozzle, by using the paired scanning magnets in horizontal (X) and vertical (Y) directions. Proton beam spot is moved around the isocenter with energies between 70–235 MeV [12]. The advantage of this technique against scattering-based technique is that a range shifter is not required to shape the beam to the tumor volume, because the synchrotron accelerate the protons slowly and conform the tumor dose in the dimension lateral to the beam [12]. The system characteristics are listed in table 1. Dose delivered to the phantom is monitored in real time by using two parallel-plate ionization chambers. Spot size and beam optic are measured by using the position detectors. Unlike discrete scan mode (pixel scan), IONTRIS provided a continuous beam scan mode (raster scan).

Table 1. The characteristics of SAPT proton therapy system obtained from [12].

Item	value
Energy (MeV)	70.0–235.0
Field size (cm^2)	30.0×40.0
Scanning magnet x to isocenter distance (cm)	287.0
Scanning magnet y to isocenter distance (cm)	242.0
Nozzle to isocenter distance (cm)	40.0
Average scan speed in x (cm/ms)	2.0
Average scan speed in y (cm/ms)	0.5
Max Dose rate (Gy/min)	2.0

2022 JINST 17 P09008

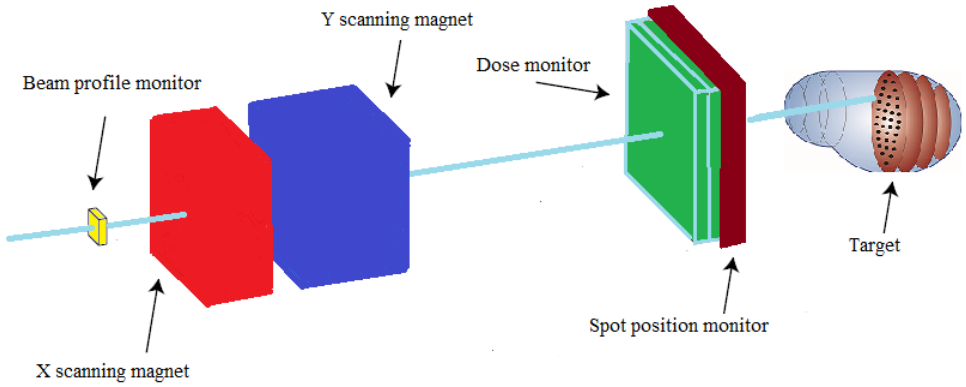

Figure 1. A schematic view of SAPT nozzle.

Passive scattering system geometry was obtained from [13]. In this design, proton beam passes through the vacuum window, first scatterer, first monitor, range modulator wheel, second scatterer, second monitor, collimator, and the size-changeable snout (brass tube). The first scatterer is set for spreading the beam laterally and the range modulator wheel spread the beam longitudinally. Two jaws can provide a size-changeable treatment field, while the aperture can control the lateral conformity of the beam.

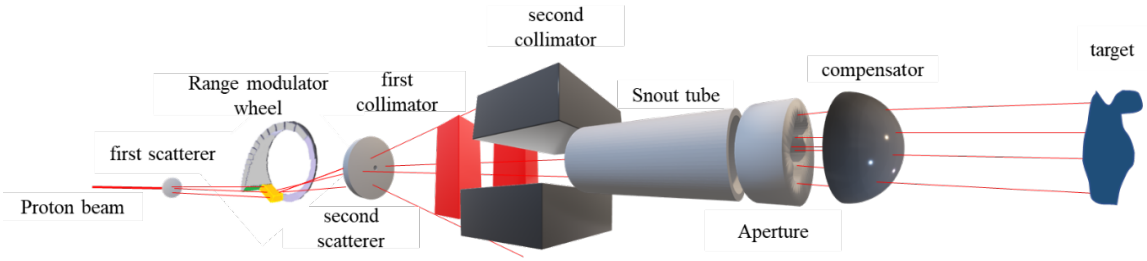

Figure 2. A schematic view of passive scattering system simulated in GATE MC code (aperture and compensator are located in the snout, in real) [13].

The strategy reported by Grevillot et al. [14] has been adopted for PBS system simulation. a complete treatment plan in GateSourceTPSPencilBeam that developed for single pencil beam for clinical application [15]. This source including two main components: source description file that describe the beam delivery system, and plan description that contain the position of spot for irradiation, magnets position, and monitor unit (MU) [14–16]. In PBS simulation, the source description file defines the beam delivery system with a set of the polynomial equations which allows calculation of the optical and energy properties of each pencil beam at the nozzle output as a function of beam energy. It consists of eight equations; where, two equations describe energy properties and the rest of the equations describe optical properties. The plan description file contains one or more fields described by gantry angle and a set of pencil beams.

In PSPT design, Northeast Proton Therapy Center (NPTC) system based on the compact 235 MeV isochronous cyclotron, was considered.the simulated geometry consists of a nozzle and a water phantom (figure 2) [13]. The system characteristics including the nozzle components and

2022 JINST 17 P09008

Table 2. Specifications of simulated PSPT nozzle [13].

Component	Material	characteristic
beam		Pencil beam, single energy
Spot size		3 mm-mrad
First scatterer	lead/Lexan[a]	Foil/ circle
First scatterer thickness		0.003–0.548 cm
second scatterer	Bi-material (lead/Lexan)	
Range modulator wheel	Lead or Lexan/carbon	
First collimator	nickel	
second collimator	Brass[b]/Myler	
snout	Brass	cylindrical
Aperture	Lucite	Patient specific[c]
compensator	Lucite	Patient specific

[a] Lexan (1.2 gr/cm^3) is composed of 5.5% H, 75.6% C and 18.9% O.
[b] Brass (8.49 gr/cm^3) is composed of 61.5% Cu, 35.2% Zn and 3.3% Pb.
[c] Internal and external dimensions vary depending on the therapeutic.

materials, are listed in table 2. All the components are simulated in mm accuracy, no ripple filter are included. For the proton beam, the mean primary energy was set on 190.027 MeV, with a Gaussian distribution of 3.5%. The scatterer thickness needs to be determined to generate a uniform proton radiation field, based on previous studies [17–22], we chose a scatterer thickness of 2.3 mm and 2.5 mm at the energies 179.9 MeV and 190.028 MeV, respectively, which resulted in a uniformity of less than 2% in the dose distribution.

In this study, two independent MC-based simulators for PBS and PSPT have been developed and benchmarked against experimental measurements reported in the literature. GATE MC code, is a multipurpose MC code based on the libraries of the Geant4 toolkit, has been used in this simulation [11]. The physical list selected for proton transport simulation is QGSP-BIC-EMZ. In addition, different values for ionization potential of water have been reported to directly influence the simulation results [23]. The value of the mean excitation energy for water, recommended in the ICRU report 90 (I = 78 ev) was adopted [24–26].

In addition, the maximum step limiter of protons was set to 0.1 mm in the water, and TG-119. Also in the simulations, for measuring the lateral profile, a grid dimension was set on the 2 mm^2, whereas it was set to 0.1 mm for Z axis (in depth) to measuring the IDD curve.

2.2 Clinical phantom study

The clinical test suite recommended by TG-119 includes structures for prostate, head and neck (H&N), and C-shape cases. The prostate phantom, uses the CTV, PTV, rectum, and bladder; the head & neck case, includes the PTV, cord, and parotide (left and right); and the C-shape phantom uses a PTV, and a core structure. The PTV in C-shape phantom wrapped around a core, whose outer surface is 5 mm from the inner surface of the PTV [27].

2022 JINST 17 P09008

2.3 Plan description

For a given radiation field, there are two main objectives: maximizing the uniform dose at the target and minimizing the non-target dose [28]. Inverse planning algorithm proposed by Sánchez et al. [29] applied for spot and beam selection. The objective function and target in this optimization was set according to the TG-119 report [30] and other references [29, 31, 32]. The accuracy of the dose volume histogram obtained from GATE simulation was benchmarked against the results reported by Sánchez et al. [29]. Hence, clinically relevant dosimetric parameters were compared in terms of mean relative error using eq. (2.1):

$$\mathrm{MRE} = \left(\frac{D_i - D_i'}{D_i}\right) \times 100 \tag{2.1}$$

where, D_i represents the dose parameters from our simulation and D_i' represents the reference data.

For the TG-119 C-shape phantom the dose goals were set base on the PTV (D95 = 50 Gy, D10 < 55 Gy), and for core (D10 < 10 Gy). A single proton field with energy between 70–104 MeV was set on the target to maximize the biological effect [29]. For H&N case 50 GyRBE dose (in 25 fraction) was prescribed to be delivered to the PTV70 (D_{20} < 55 GyRBE, D_{99} < 46.5 GyRBE, and D_{90} = 50 GyRBE). While maximum dose goal to the OARs were restricted as following: dose to the cord (max < 50 GyRBE), brain stem (max < 54 GyRBE) and for parotide (D_{50} < 20 GyRBE). To minimize the biological effect on non-target volumes, two field with 50, and 310 degree angles and the proton energy between 102–182 MeV were set [29, 31]. In the prostate case, prescribe dose was selected 80 GyRBE (in 40 fraction) [29, 32], with the goal dose to PTV (D_5 < 83 Gy, and D_{95} > 75.6 Gy). Dose to rectum was set to $V70_{\mathrm{GyRBE}}$ < 30% and $V50_{\mathrm{GyRBE}}$ < 60%. Dose to bladder was restricted by $V70_{\mathrm{GyRBE}}$ < 35%, $V50_{\mathrm{GyRBE}}$ < 60%, and for femur it was defined $V50_{\mathrm{GyRBE}}$ < 5%. Two parallel opposed proton field with energy range of 130–160 MeV was used to minimize the dose effect on the normal tissue. During the planning, relative biological effect of protons was applied by a constant factor of 1.1. Also, all the mentioned simulations are performed with a PC with core i7 CPU and 16 GB RAM.

2.4 Quantitative analysis

Both PSPT and PBS facilities were benchmarked against experimental data in terms of depth dose curve and SOBP plan. The average point-to-point[1] difference between each series of data were calculated. When the MC simulators of two systems have been validated, they were compared under the same simulation parameters using water phantom and TG-119 test cases. The physical dose parameters including BP_{W50}, peak location, range, peak-to-entrance dose ratio, $\mathrm{penumbra}_{(90-10)\%}$,[2] and $\mathrm{penumbra}_{(80-20)\%}$[3] were compared. In addition, based on the SOBP plan, the factor of conformity, $M_{95\%}$, entrance dose, $\mathrm{penumbra}_{(90-10)\%}$, and $\mathrm{penumbra}_{(80-20)\%}$ were compared. Furthermore, DVH-driven clinical parameters obtained from TG-119 simulation were compared between two proton therapy techniques. Also, for comparison of the parameters including BP_{W50}, peak location, range,

[1] $\omega = \sum_{i=1}^{N} \left(\frac{|d_i - d_{\mathrm{ref}i}|}{d_{\mathrm{ref}i}} \times \frac{\Delta}{L}\right)$ Where d_i and $d_{ref\,i}$ refers to the simulation and measurement, Δ is the step between two point, and L is the maximum range.

[2] $\mathrm{penumbra}_{(90-10)\%}$: distal falloff of dose from 90% to 10%.

[3] $\mathrm{penumbra}_{(80-20)\%}$: distal falloff of dose from 80% to 20%.

2022 JINST 17 P09008

peak-to-entrance dose ratio the related parameter for PBS mode was selected as a reference for computing the mean relative error using eq. (2.2):

$$\mathrm{MRE} = \left(\frac{x_{\mathrm{pbs}} - x_{\mathrm{pspt}}}{x_{\mathrm{pbs}}}\right) \times 100 \tag{2.2}$$

where, x_{pbs} represents the parameters (listed above) from our simulation of PBS mode, and x_{pspt} represents the represents the parameters from our simulation of PSPT mode.

3 Results and discussion

3.1 Experimental study

Figure 3 shows a comparison between the simulated and the experimental data in the term of Integrated Depth Dose (IDD) at the energy of 161.1 MeV (at the beginning of the nozzle) and SOBP curve for PBS system, and the experimental data obtained from [12, 13]. The simulation results illustrate a good agreement with the experimental measurements. For each IDD curve, the simulation time for 10^5 incident protons, approximately was 385 second. Also, for the SOBP curve the number of primary particles was 0.5×10^8, so the computation time approximately raised to 2.286×10^3 seconds.

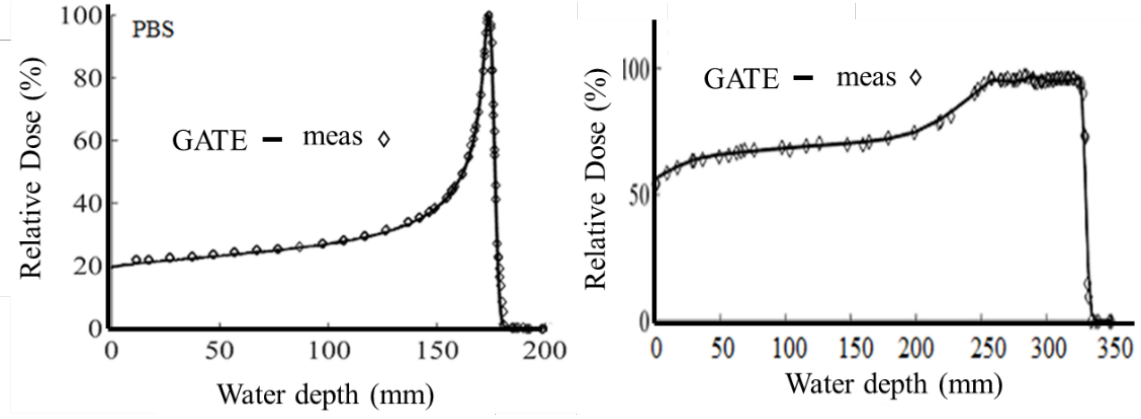

Figure 3. Comparison between the simulated and experimental data for IDD parameters (right), and SOBP curve (left) in the active scan-based method.

Figure 4. Demonstrates a good agreement between the simulated data and experimental data for both IDD in the energy of 190.027 MeV, and SOBP curves in PSPT technique. In the term of IDD curve, For the PBS system, the mean point-to-point difference between the simulation and measurement was 1.5%, while for PSPT system the mean point-to-point difference was calculated about 2.76%. also, in the SOBP curve, the mean relative error for PBS was calculate about 0.97% while for PSPT was 1.08%.

Figure 5 compares the simulated Bragg peak location, range (R80), BP_{W50} and peak-to-entrance dose ratio between PBS and PSPT beam delivery methods in different energies under the same conditions. Bragg-peak location between the two methods had a mean relative difference of 0.74% with a maximum difference of 0.99%. Accordingly, no significant difference on the energy discharge

2022 JINST 17 P09008

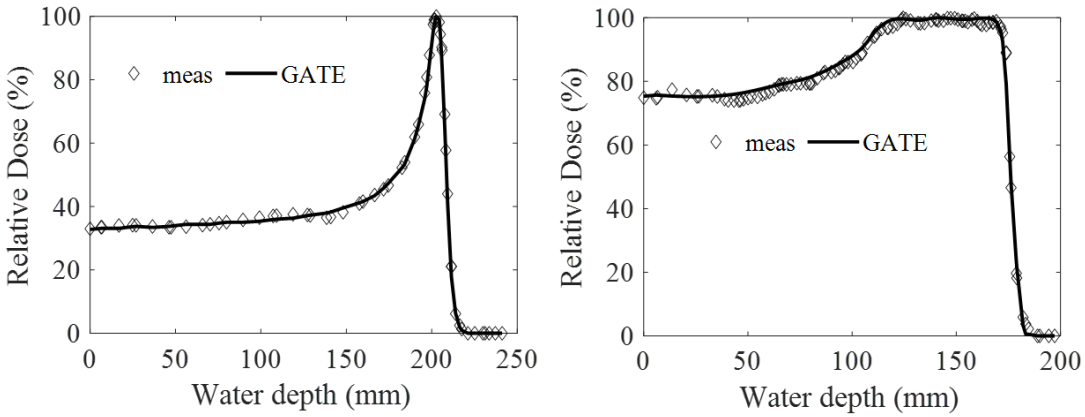

Figure 4. Comparison between the simulated and experimental data for IDD parameters (left), and SOBP curve (right) in the scattering-based method.

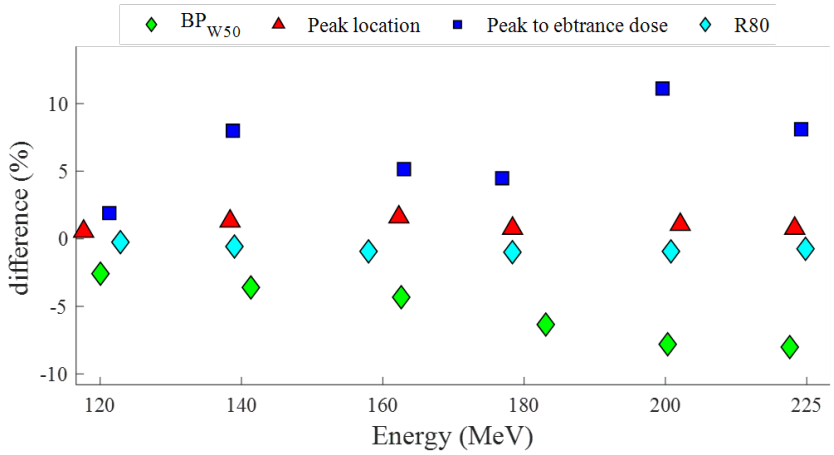

Figure 5. Comparison between two modes of PT, in all terms the PBS related parameter considered as a reference.

location has been observed between two methods. The parameter of proton beam range in the scattering is slightly longer than the active scanning method with an average difference of 1.8 mm (maximum difference 2.9 mm). In addition, comparison of BP_{W50} parameter between scattering system versus active scanning technique show a considerable difference of about 8%. The ratio of peak to entrance dose (normalized) is considerably higher with an average difference of 6.45% (ranging between 1.9–11.11%) in PSPT compared to PBS.

SOBP plan and depth-dose curve in water phantom under the same conditions are compared between PBS and PSPT in Fig 6. The mean relative difference in IDD profile between two methods was calculated about 9.3%. In PSPT mode, the slope of the fall-off[4] in SOBP curve (normalized) is −0.03 and in PBS mode the slope of the fall-off is −0.08. The physical range extracted from SOPB

[4]Slope of distal falloff is the slope of decrease from distal 80% to distal 20% in the depth dose curve.

2022 JINST 17 P09008

curve in the passive scattering method (354.73 mm) compared to PBS mode (353.37 mm) is about 1.36 mm larger. In addition, the value of discharged dose in the modulation region for PBS mode is about 4% higher than that calculated in PSPT mode. The entrance dose in PBS mode (0.51) was lower by a factor of 17.34% compared to simulated passive scattering design (0.617). the values of penumbra$_{(90-10)\%}$ and penumbra$_{(80-20)\%}$ are compared between to method in IDD curve and SOBP curve, in IDD curve the value of penumbra$_{(90-10)\%}$ in PSPT system is 1.2 mm larger than this value for PBS system, also the value of penumbra$_{(80-20)\%}$ is 0.5 mm larger in PSPT compared to PBS design. For the SOBP curve, For the SOBP curve, the value of $M_{95\%}$ in the PSPT system is 2.8 mm larger than that obtained from PBS system. In term of penumbra$_{(90-10)\%}$, penumbra$_{(80-20)\%}$, there is 10.2 mm and 4.6 mm difference between two methods, respectively. Also, the mean point-to-point parameter was used to compare the plateau region of SOBP curve, we select two points in start and stop of the plateau region (on the $M_{95\%}$), the comparison shows the 0.57% difference between two methods.

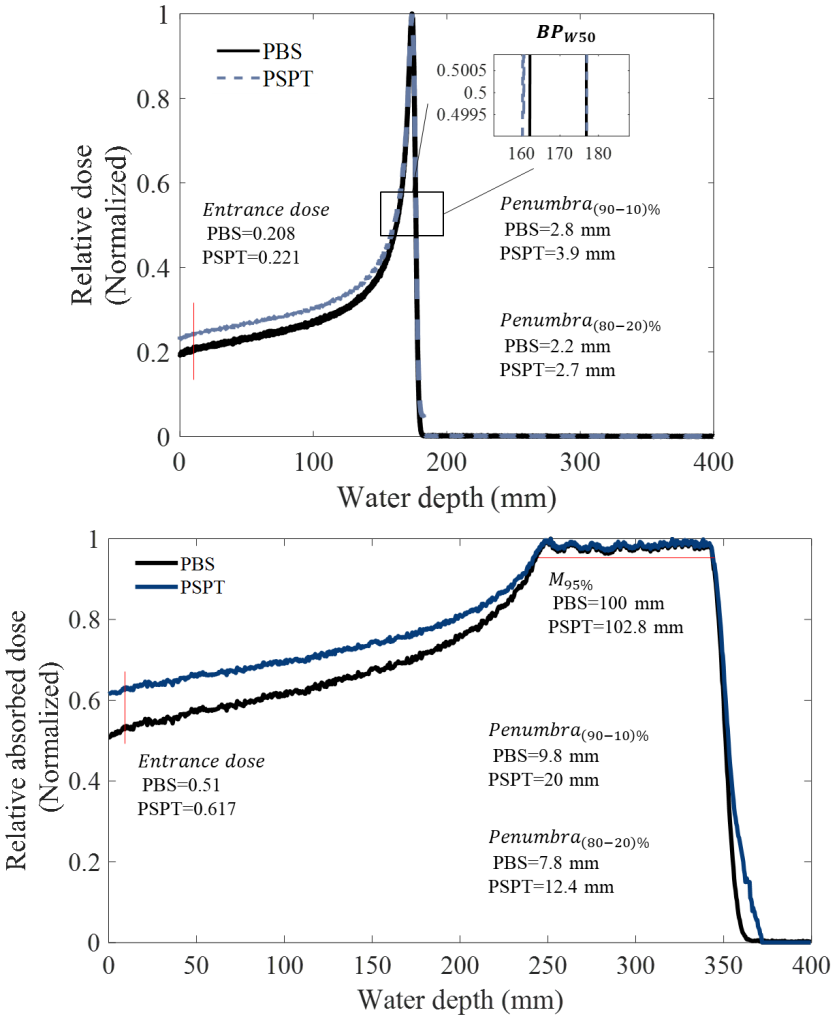

Figure 6. IDD (top) in proton energy of 159.9 MeV, and SOBP (down) diagram obtained from simulated PBS and PSPT systems in.

2022 JINST 17 P09008

3.2 Clinical study

Dose distribution for TG-119 phantoms in the pencil beam scanning proton therapy compared to passive scattering model along with DVH analysis for targets and OARs are illustrated in figures 7 and 8. The clinically relevant dose parameters between two modes of proton therapy have been compared in table 3. The results showed that the difference of PTV mean dose between PBS and PSPT techniques are up to 1.8% while the difference of max dose to organ at risks (OARs) exceeds 50% for the spinal cord in H&N case-study. Also, the calculation time in these cases varied between 25.2 hours and 31 hours, according to the dose level defined for each case (1.66 Gy for C-shape target, and 2 Gy for H&N and prostate test case (in each fraction)).

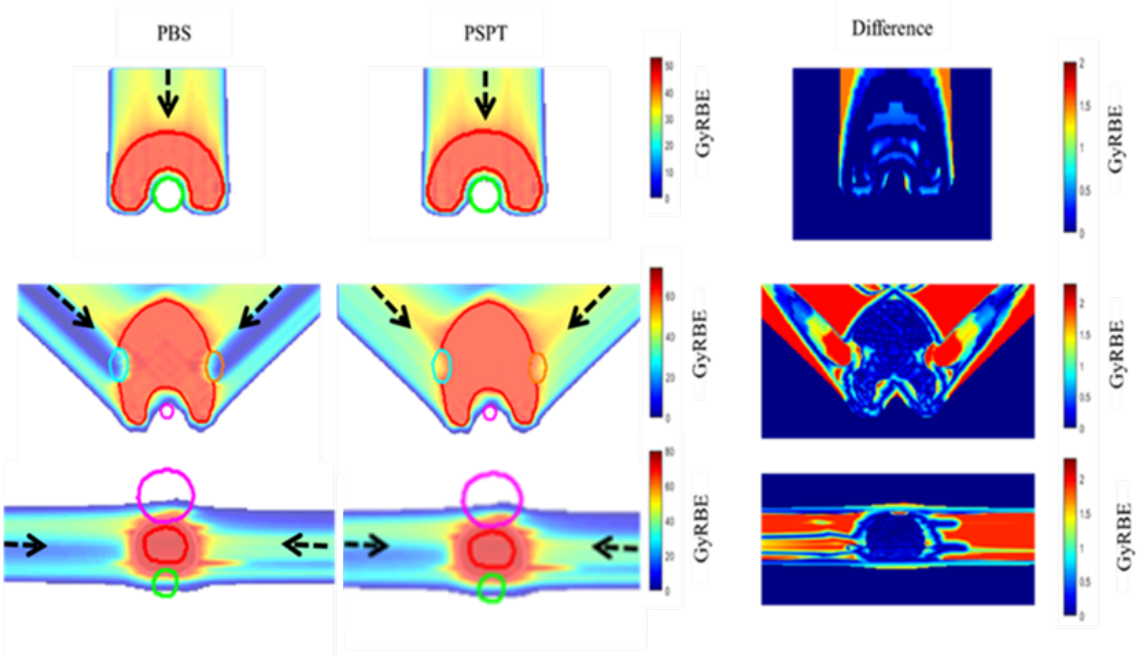

Figure 7. 3D dose distribution and comparison for PBS and PSPT plans (The arrow indicates the direction of the incoming beam).

4 Discussion and conclusion

Nowadays, the treatment of cancerous tumors by particles is increasing due to their outstanding features in the delivery of tailors. In this study, the main methods of beam delivery in proton therapy were simulated, and essential quantities such as peak Bragg location, range, BP_{W50}, the ratio of dose at peak to input, and SOBP on the target volume in a cubic water phantom were evaluated at different energies. Furthermore, the DVH analysis based on the clinical TG-119 test cases have been investigated. According to our results, some advantages in terms of physical dose parameters in active scanning model compared to passive scattering mode has been observed. However, factor of proton range and peak location were not significantly different between the two nozzle designs. A sharper slope of fall-off in SOBP curve was observed in PBS mode compared to PSPT enabling a more controllable performance to adapt dose to the target volume; where, the sharper the curve, the higher

2022 JINST 17 P09008

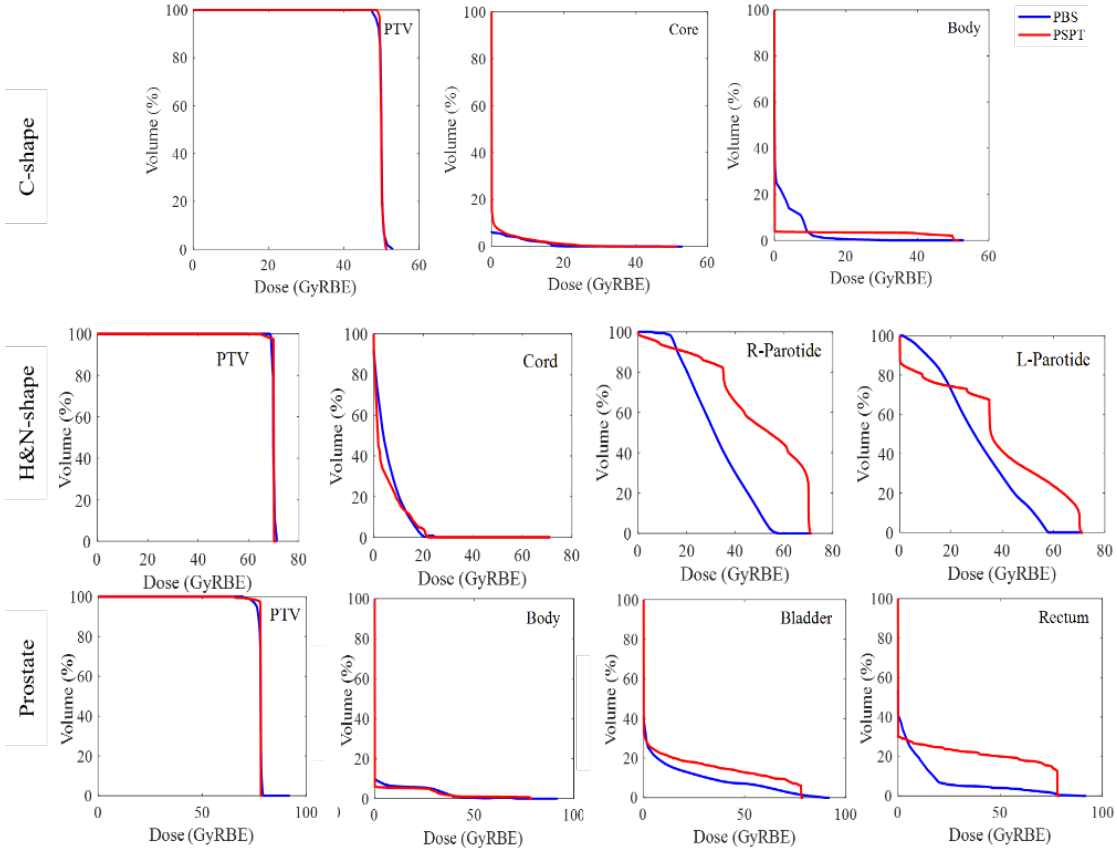

Figure 8. DVH analysis for PBS (blue line) and PSPT (red line) plans.

the beam control and the better the dose adjustment on the target area. BP_{W50} in depth-dose profile was on average 8% larger in scattering system compared to active scanning mode which stems from scattering events and secondary particle generation in the trajectory of proton beam. The ratio of peak-to-entrance dose within the target volume was another investigated quantity in the present work. By comparing this quantity, we found that the inactive dispersion of the transmitters deposited in the skin and surrounding healthy tissue was significantly lower in the active scanning method. The total deposited energy in the out-of-modulation region in PSPT was about 20% higher than PBS mode (figure 6, area under SOBP curve); which is an important advantage of PBS in clinical application, also the penumbra region in the PBS system is much lower than that for PSPT system (figure 6),which can lead to better control over the target volume, lower uncertainties and improving the quality of treatment. It can be seen that in the active scanning method, the tumor volume can be better covered and less stitches can be delivered to healthy tissues. Based on the DVH-driven parameters (table 3), it can be seen that the capability of the PBS mode to reduce the dose to non-target volumes is superior to PSPT while the total dose to body contour is reduced in average about 29.9% in three TG-119 test cases. In the high dose region of bladder in prostate DVH that is quantified by V75, V70 and V65 indices, the outperformance of PBS versus PSPT has been illustrated. In addition, better conformity of dose to PTV is observed from the fall-off slope in DVH analysis (figure 8).

2022 JINST 17 P09008

Table 3. Dose parameter obtained from dose volume histogram data

Phantom	Organ	Indices	PSPT	PBS	Dif (%)
C-shape	PTV	Mean dose (Gy)	50.4	49.5	-1.8
		max dose (Gy)	53.7	53.1	−1.1
		D 98% (Gy)	49.2	48.9	−0.61
		D 95% (Gy)	49.5	50.1	1.2
		D 50% (Gy)	51.45	51.45	0
		D 2% (Gy)	52.1	52.2	0.2
	Core	Mean dose (Gy)	5.21	4.177	−1.03
		Max dose (Gy)	33.06	19.751	−13.3
		Min dose (Gy)	0	0	0
Prostate	Bladder	V80	0	0	0
		V75	7.161	2.6	−4.56
		V70	9.33	3.6	−159.1
		V65	9.71	4.5	−115.7
	Rectum	V75	14.92	6.28	−137.5
		V70	16.75	8.50	-97
		V65	17.63	8.73	-101.9
		V60	18.28	9.01	-102.9
	PTV	D95 (Gy)	76.7	75.44	−1.26
		D5 (Gy)	81.07	78.1	−3.8
		Mean dose (Gy)	79	77.8	−1.2
H&N	Cord	Max	13.5	9	−50
	L parotide	V30	69.5	49	−41.8
		V40	41.22	28	−47.2
	R parotide	V30	84	53	−58.4
		V40	65	29	−124.1
	PTV	D95 (Gy)	68	67.6	−0.6
		D5 (Gy)	70	70.2	0.28
		Mean dose (Gy)	70.2	69.6	−0.85

In the present study, the results of the simulation of pencil beam and scattering systems were validated against the experimental data. Therefore, we believe that the simulations performed in this study have the capability to be utilized as independent dose engine simulator of the given systems and applicable in the quality assurance process. Furthermore, under the same conditions and in a homogeneous water phantom, the quantities related to both dose and adaptability properties were investigated and the superiority of spot scanning method in both dose transfer and adaptation was investigated. According to the literature, there are some controversies regarding the distal dose of PSPT against PBS systems [3, 6, 7]; it might stem from the fact that the estimated physical/ biological dose in passive scattering proton therapy systems are dependent on the specific scattering hardware's that are implemented in the beam trajectory, in some literature, the studies were made to evaluate

2022 JINST 17 P09008

the effect of secondary product on the total dose of protons, presence of the secondary particles are estimated about 4 to 10 times higher in the scattering techniques compared to pencil beam design, however, it has been reported that their contribution in the total absorbed dose is less than 1% [33–36]. In this regard, the performance of multiple scattering designs should be simulated and further compared to provide a global conclusion about the advantages and disadvantages of active scanning proton therapy technique against passive scattering mode. In the next step, it is better to do such a study in the tissue and in conditions such as the presence of implants to clarify the importance of therapeutic methods in dose delivery (and ability of PT mode to reduce the dose of secondary products).

4.1 Acknowledgments

This work was supported by Sharif University of Technology and the Swiss National Science Foundation under grant SNRF 320030_176052.

Author Contributions. All authors contributed to the study conception and design. All authors read and approved the final manuscript.

References

[1] R.R. Wilson, *Radiological use of fast protons*, *Radiology* **47** (1946) 487.

[2] ICRU, *Prescribing, Recording, and Reporting Proton-Beam Therapy International Commission on Radiation Units and Measurements*, Tech. Rep., Report 78, Bethesda, MD, U.S.A. (2007).

[3] A. Michaelidesová, J. Vachelová, J. Klementová, T. Urban, K.P. Brabcová, S. Kaczor et al., *In vitro comparison of passive and active clinical proton beams*, *Int. J. Mol. Sci.* **21** (2020) 5650.

[4] T. Kanai, K. Kawachi, Y. Kumamoto, H. Ogawa, T. Yamada, H. Matsuzawa et al., *Spot scanning system for proton radiotherapy*, *Med. Phys.* **7** (1980) 365.

[5] T. Furukawa, T. Inaniwa, S. Sato, T. Shirai, Y. Takei, E. Takeshita et al., *Performance of the NIRS fast scanning system for heavy-ion radiotherapy*, *Med. Phys.* **37** (2010) 5672.

[6] K. Nomura, H. Iwata, T. Toshito, C. Omachi, J. Nagayoshi, S. Hashimoto et al., *Biological effects of spot scanning and passive scattering proton beams at the distal end of the spread-out bragg peak (SOBP) in single cells and multicell spheroids*, *Int. J. Radiat. Oncol. Biol. Phys.* **105** (2019) E644.

[7] D.S. Gridley, M.J. Pecaut, X.W. Mao, A.J. Wroe and X. Luo-Owen, *Biological effects of passive versus active scanning proton beams on human lung epithelial cells*, *Technol. Cancer Res. Treat.* **14** (2015) 81.

[8] D. Strulab, G. Santin, D. Lazaro, V. Breton and C. Morel, *GATE (GEANT4 application for tomographic emission): a PET/SPECT general-purpose simulation platform*, *Nucl. Phys. B Proc. Supp.* **125** (2003) 75.

[9] S. Jan, G. Santin, D. Strul, S. Staelens, K. Assié, D. Autret et al., *GATE: a simulation toolkit for PET and SPECT*, *Phys. Med. Biol.* **49** (2004) 4543.

[10] OpenGATE collaboration, *GATE Users Guide.*, https://opengate.readthedocs.io/en/latest/.

[11] S. Jan, D. Benoit, E. Becheva, T. Carlier, F. Cassol, P. Descourt et al., *GATE v6: a major enhancement of the GATE simulation platform enabling modelling of CT and radiotherapy*, *Phys. Med. Biol.* **56** (2011) 881.

[12] H. Shu, C. Yin, H. Zhang, M. Liu, M. Zhang, L. Zhao et al., *Scanned proton beam performance and calibration of the shanghai advanced proton therapy facility*, *MethodsX* **6** (2019) 1933.

2022 JINST 17 P09008

[13] H. Paganetti, H. Jiang, S.-Y. Lee and H.M. Kooy, *Accurate Monte Carlo simulations for nozzle design, commissioning and quality assurance for a proton radiation therapy facility*, *Med. Phys.* **31** (2004) 2107.

[14] L. Grevillot, D. Bertrand, F. Dessy, N. Freud and D. Sarrut, *A Monte Carlo pencil beam scanning model for proton treatment plan simulation using GATE/GEANT4*, *Phys. Med. Biol.* **56** (2011) 5203.

[15] L. Grevillot, D. Bertrand, F. Dessy, N. Freud and D. Sarrut, *GATE as a GEANT4-based Monte Carlo platform for the evaluation of proton pencil beam scanning treatment plans*, *Phys. Med. Biol.* **57** (2012) 4223.

[16] R. Gaizauskas et al., *GATE User Guide*, 1996.

[17] U. Titt, Y. Zheng, O.N. Vassiliev and W.D. Newhauser, *Monte Carlo investigation of collimator scatter of proton-therapy beams produced using the passive scattering method*, *Phys. Med. Biol.* **53** (2007) 487.

[18] E. Grusell, A. Montelius, A. Brahme, G. Rikner and K. Russell, *A general solution to charged particle beam flattening using an optimized dual-scattering-foil technique, with application to proton therapy beams*, *Phys. Med. Biol.* **39** (1994) 2201.

[19] M. Engelsman, H.-M. Lu, D. Herrup, M. Bussiere and H.M. Kooy, *Commissioning a passive-scattering proton therapy nozzle for accurate SOBP delivery*, *Med. Phys.* **36** (2009) 2172.

[20] T. Aso, A. Kimura, S. Tanaka, H. Yoshida, N. Kanematsu, T. Sasaki et al., *Verification of the dose distributions with GEANT4 simulation for proton therapy*, *IEEE Trans. Nucl. Sci.* **52** (2005) 896.

[21] K. Chung, J. Kim, D.-H. Kim, S. Ahn and Y. Han, *The proton therapy nozzles at Samsung Medical Center: A Monte Carlo simulation study using TOPAS*, *J. Korean Phys. Soc.* **67** (2015) 170.

[22] S. Hang, F. Shou-Xian, G. Xia-Ling, T. Jing-Yu, L. De-Kang, F. Shi-Nian et al., *Irradiation methods and nozzle design for the advanced proton therapy facility*, *Chin. Phys. C* **34** (2010) 516.

[23] N. Zahra, T. Frisson, L. Grevillot, P. Lautesse and D. Sarrut, *Influence of Geant4 parameters on dose distribution and computation time for carbon ion therapy simulation*, *Phys. Med.* **26** (2010) 202.

[24] C. Winterhalter, M. Taylor, D. Boersma, A. Elia, S. Guatelli, R. Mackay et al., *Evaluation of GATE-RTion (GATE/Geant4) Monte Carlo simulation settings for proton pencil beam scanning quality assurance*, *Med. Phys.* **47** (2020) 5817.

[25] L. Grevillot, J.O. Moreno, V. Letellier, R. Dreindl, A. Elia, H. Fuchs et al., *Clinical implementation and commissioning of the MedAustron Particle Therapy Accelerator for non-isocentric scanned proton beam treatments*, *Med. Phys.* **47** (2019) 380.

[26] A. Elia, A.F. Resch, A. Carlino, T.T. Böhlen, H. Fuchs, H. Palmans et al., *A GATE/Geant4 beam model for the MedAustron non-isocentric proton treatment plans quality assurance*, *Phys. Med.* **71** (2020) 115.

[27] D.K. Mynampati, R. Yaparpalvi, L. Hong, H.-C. Kuo and D. Mah, *Application of AAPM TG 119 to volumetric arc therapy (VMAT)*, *J. Appl. Clin. Med. Phys.* **13** (2012) 108.

[28] F. Bourhaleb, F. Marchetto, A. Attili, G. Pittà, R. Cirio, M. Donetti et al., *A treatment planning code for inverse planning and 3D optimization in hadrontherapy*, *Comput. Biol. Med.* **38** (2008) 990.

[29] D. Sánchez-Parcerisa, M. López-Aguirre, A.D. Llerena and J.M. Udías, *MultiRBE: Treatment planning for protons with selective radiobiological effectiveness*, *Med. Phys.* **46** (2019) 4276.

[30] G.A. Ezzell, J.W. Burmeister, N. Dogan, T.J. LoSasso, J.G. Mechalakos, D. Mihailidis et al., *IMRT commissioning: Multiple institution planning and dosimetry comparisons, a report from AAPM Task Group 119*, *Med. Phys.* **36** (2009) 5359.

2022 JINST 17 P09008

[31] A. Montero, M. Martín, eds., *Manual Práctico de Oncología Radioterápica*, Grupo Editorial abbvie, Madrid (2013).

[32] N.P. Mendenhall, Z. Li, B.S. Hoppe, R.B. Marcus, W.M. Mendenhall, R.C. Nichols et al., *Early outcomes from three prospective trials of image-guided proton therapy for prostate cancer*, *Int. J. Radiat. Oncol. Biol. Phys.* **82** (2012) 213.

[33] H. Paganetti, *Nuclear interactions in proton therapy: dose and relative biological effect distributions originating from primary and secondary particles*, *Phys. Med. Biol.* **47** (2002) 747.

[34] U. Schneider, S. Agosteo, E. Pedroni and J. Besserer, *Secondary neutron dose during proton therapy using spot scanning*, *Int. J. Radiat. Oncol. Biol. Phys.* **53** (2002) 244.

[35] S. Agosteo, C. Birattari, M. Caravaggio, M. Silari and G. Tosi, *Secondary neutron and photon dose in proton therapy*, *Radiother. Oncol.* **48** (1998) 293.

[36] P. Binns and J. Hough, *Secondary dose exposures during 200 MeV proton therapy*, *Radiat. Protect. Dosim.* **70** (1997) 441.

2022 JINST 17 P09008